J. Fluid Mech. (1981), *vol.* 110, *pp.* 129–147
Printed in Great Britain

Interaction between a vortex filament and an approaching rigid sphere

By M. R. DHANAK
Department of Mathematics, Imperial College, London

(Received 10 October 1980)

The evolution of an infinitely long straight vortex filament in the presence of an approaching rigid sphere is considered. The fluid is regarded as being inviscid and incompressible. The shape of the vortex filament when the sphere is sufficiently far away from the vortex is determined approximately using linear theory. The subsequent evolution is followed numerically by integrating the nonlinear equation of motion.

1. Introduction

In consideration of vortex filaments in inviscid flow, it is often of interest to determine how these interact with each other or with surfaces present in the flow field. The trailing vortices of an aircraft and a vortex ring approaching a rigid wall are examples of such interactions. Raja Gopal (1963) has considered the motion of a vortex ring in a circular cylinder while Crow (1970) and Moore (1972) have looked at growth of waves on the trailing vortices of an aircraft. This paper is concerned with the interaction between a vortex filament and a moving bluff body.

A rigid sphere can in many ways be regarded as a typical bluff body and the particular case considered here is when the sphere approaches an infinitely long straight vortex from infinity at a uniform speed. The evolution of the vortex is studied. The fluid is regarded as being inviscid and incompressible and of uniform density.

The motion of the vortex is symmetrical about a plane which passes through the centre of the sphere and whose normal is parallel to the axis of the undisturbed straight vortex. Thus the situation considered is equivalent to the case of a vortex filament moving in a uniform stream over a rigid plane with a hemispherical hump in its path.

The vortex is regarded as having a small circular cross-section of core radius c. This is justified provided that the strain-field to which the vortex is subjected is sufficiently small (Moore & Saffman 1971).

In order to follow the motion of the vortex, the approximate velocity at the vortex is obtained using the cut-off theory, due to Crow (1970). Then the Helmholtz law, that in inviscid fluid vortex lines move with the fluid, lead to an integro-differential equation for the motion of the vortex filament.

The cut-off theory, wherever possible, treats the vortex as being of zero cross-section and the velocity field due to the vortex is calculated using the Biot–Savart line integral. However, the integral diverges on the vortex line itself. The difficulty is overcome by means of a 'cut-off', the choice of which depends on the structure of the vortex filament, i.e. its core radius and the radial distribution of vorticity (as well as axial flow

if present). The influence of the internal structure on the motion of the vortex enters only through the cut-off.

A rigorous justification for the cut-off theory has been provided by Widnall, Bliss & Zalay (1971) and Moore & Saffman (1972). The latter give a rule for estimating the instantaneous area of the filament cross-section; the variation of the area cannot be ignored in nonlinear calculations. It can be shown that the velocity at the axis of the vortex is approximately that defined by a suitable cut-off. In the absence of axial flow in the filament, which is the case to be considered here, the error in the velocity defined by the cut-off theory is $O(c^2/\rho^2)$, where c is the core radius and ρ is a typical radius of curvature (the error is $O(c/\rho)$ when axial flow is present, owing to the effect of Coriolis and Reynolds stress forces). The cut-off method is described more fully later.

The problem is considered in two stages. When the sphere is at a large distance away from the vortex, the interaction between the vortex and the sphere is weak so that the evolution can be approximately determined using linear theory. Thus in § 2 the equation of motion of the filament is linearized and solved to obtain an expression for the shape of the vortex; the disturbance velocity due to the approaching sphere is evaluated using spherical harmonic analysis.

The shape of the vortex given by linear theory is evaluated at a time when the sphere, approaching at a uniform speed, is at a prescribed distance away from the position of the undisturbed vortex. This is used as the starting configuration for the nonlinear marching problem (2.4) which is integrated numerically for subsequent times. In § 3, the numerical procedure used in the calculations is described while, in § 4, the image system of a vortex element in a sphere, due to Lighthill (1956), is described and an expression for the velocity contribution at the vortex due to the image system is obtained for use in the numerical calculations.

The numerical results are presented in § 5. The neglect of viscous diffusion and the wake of the sphere means that the results are of only approximate validity in real fluid flows. Indeed, a qualitative experiment with a bathtub vortex shows that although the vortex commences to move as anticipated in § 5, when the sphere is close to the vortex, the wake appears to interact strongly with the vortex.

2. Equation of motion and linear theory

Let rectangular axes $Oxyz$ be chosen so that, in the undisturbed state, Oz lies along the axis of the vortex filament. If the vortex has strength Γ and if at time t^* its axis occupies the curve given parametrically by $\mathbf{X}^*(\xi, t^*)$, where ξ is chosen so that ξ = constant always refers to the same fluid particle, then its motion is governed by

$$\frac{\partial \mathbf{X}^*(\xi,t^*)}{\partial t^*} = \frac{\Gamma}{4\pi} \oint_{-\infty}^{\infty} \frac{\partial \mathbf{X}^*(\xi,t^*)}{\partial \xi} \wedge \frac{(\mathbf{X}^*(\xi_0,t^*) - \mathbf{X}^*(\xi,t^*))\, d\xi}{|\mathbf{X}^*(\xi_0,t^*) - \mathbf{X}^*(\xi,t^*)|^3} + \mathbf{V}_E^*(\xi_0,t^*), \quad (2.1)$$

where $\mathbf{V}_E^*(\xi_0, t^*)$ is the contribution to the velocity at ξ_0 due to the image vorticity in the sphere and due to the motion of the sphere. The notation $\oint$ implies that a suitable cut-off is used to make the line integral finite at $\xi = \xi_0$. If the radius of the sphere is a and its speed is U, then (2.1) can be non-dimensionalized by choosing

$$\mathbf{X}^* = a\mathbf{X}, \quad t^* = \frac{4\pi a^2}{\Gamma} t, \quad \mathbf{V}_E^* = U\mathbf{V}_E, \quad (2.2)$$

as well as writing the arc distance $s^*(\xi, t^*)$ along the filament and core radius c^* as

$$s^* = as, \quad c^* = ac. \tag{2.3}$$

Then

$$\frac{\partial \mathbf{X}(\xi,t)}{\partial t} = \oint_{-\infty}^{\infty} \frac{\partial \mathbf{X}(\xi,t)}{\partial \xi} \wedge \frac{(\mathbf{X}(\xi_0,t)-\mathbf{X}(\xi,t))\,d\xi}{|\mathbf{X}(\xi_0,t)-\mathbf{X}(\xi,t)|^3} + \frac{\mathbf{V}_E(\xi_0,t)}{B}, \tag{2.4}$$

where

$$B = \frac{\Gamma}{4\pi a U}. \tag{2.5}$$

The value of B determines the relative importance in $\mathbf{V}_E$ of the contribution due to the image vorticity and that due to the motion of the sphere.

Two methods of cut-off to deal with the divergence of the self-induced velocity integral in (2.4) are used. For the linear analysis, the method of cut-off employed is that due to Crow (1970). This requires that a portion $(\xi_0-\epsilon, \xi_0+\epsilon)$ be removed from the range of integration, ϵ being chosen so that $|s(\xi_0+\epsilon,t)-s(\xi_0-\epsilon,t)| = 2\delta_c c$, where δ_c is a constant determined by evaluating the velocity of a circular vortex ring using the cut-off integral and comparing it with the known exact result given by Saffman (1970). This gives

$$\ln 2\delta_c = \tfrac{1}{2} - \frac{1}{4}\int_0^c r_1 v^2(r_1)\,dr_1, \tag{2.6}$$

where $v^* = \Gamma v(r_1)/4\pi a$ is the swirl velocity in the core and there is no axial flow in the filament. The crucial assumption is that the cut-off length $2\delta_c c$ is independent of the geometric shape of the vortex filament and depends only on the local structure of the vortex. Thus the same value of δ_c as for a circular vortex ring can be used for a vortex filament of any shape provided their local structures are the same. For a uniform vortex $v = 2r_1/c^2$ so that

$$\ln 2\delta_c = \tfrac{1}{4}. \tag{2.7}$$

It may be noted that, since $\partial \mathbf{X}/\partial s = \hat{\mathbf{t}}$, a unit tangent vector to the vortex, it follows that $\partial s/\partial \xi = |\partial \mathbf{X}/\partial \xi|$ so that the cut-off length may be written as

$$2\delta_0 c = \int_{\xi_0-\epsilon}^{\xi_0+\epsilon} \left|\frac{\partial \mathbf{X}}{\partial \xi}\right| d\xi. \tag{2.8}$$

Equation (2.8) relates ϵ to the cut-off length. Before the cut-off length can be determined, a rule must be given for evaluating the core radius $c(\xi_0, t)$. However, for infinitesimal disturbances, the effect of variation of c from its initial value on the governing equation is of second order in the perturbation quantity so that for the linear analysis this can be neglected and, uniformly in $\xi, c = c_0$, where $c_0^* = ac_0$ is the initial value of the core radius. For finite-amplitude disturbances this variation in core size cannot be neglected and is discussed in § 3.

For convenience, the origin of time is chosen so that at $t = 0$ the centre of the approaching sphere is at the position of the undisturbed vortex. Thus $t = -\infty$ corresponds to the time when the sphere is at infinity and the vortex is straight. The parameter ξ is chosen so that

$$\mathbf{X}(\xi, -\infty) = \xi \mathbf{k}, \quad -\infty < \xi < \infty. \tag{2.9}$$

At subsequent times ξ = constant will always represent the same fluid particle.

For an infinitesimal disturbance to the vortex, the parametric equation of the perturbed vortex is taken as

$$\mathbf{X}(\xi,t) = (\xi\mathbf{k} + \alpha\mathbf{x}'(\xi,t) + O(\alpha^2)), \tag{2.10}$$

where $\alpha \ll 1$. α measures the amplitude of the response of the vortex. The external velocity field $\mathbf{V}_E$ must also be expanded in terms of α. Thus

$$\mathbf{V}_E(\xi,t) = \alpha\mathbf{V}'_E(\xi,t) + O(\alpha^2). \tag{2.11}$$

Substituting (2.10) and (2.11) into (2.4) and retaining terms to order α only gives

$$\frac{\partial\mathbf{x}'(\xi_0,t)}{\partial t} = \mathbf{k}\wedge\int_{\substack{-\infty\\[\delta_c]}}^{\infty} \frac{\mathbf{x}'(\xi_0,t)-\mathbf{x}'(\xi,t)-(\xi_0-\xi)\,\partial\mathbf{x}'(\xi,t)/\partial\xi\,d\xi}{|\xi_0-\xi|^3} + \frac{\mathbf{V}'_E(\xi_0,t)}{B}, \tag{2.12}$$

where $[\delta_c]$ implies Crow's cut-off method. In view of (2.8) and the constancy of the core radius

$$\delta_c c_0 = \epsilon(1+O(\alpha)). \tag{2.13}$$

To solve (2.12) for a given $\mathbf{V}'_E$, the Fourier transform of the equation with respect to ξ_0 is taken. Thus, writing

$$\hat{\mathbf{x}}(k,t) = \int_{-\infty}^{\infty} \mathbf{x}'(\xi_0,t)\,e^{ik\xi_0}d\xi_0, \quad \hat{\mathbf{V}}_E(k,t) = \int_{-\infty}^{\infty} \mathbf{V}'_E(\xi_0,t)\,e^{ik\xi_0}d\xi_0, \tag{2.14}$$

the transform equation, after a change in variable of the cut-off integral, becomes

$$\frac{\partial\hat{\mathbf{x}}(k,t)}{\partial t} = \mathbf{k}\wedge\int_{-\infty}^{\infty} e^{ik\xi_0}d\xi_0 \int_{\substack{-\infty\\[\delta_c]}}^{\infty} \frac{\mathbf{x}'(\xi_0,t)-\mathbf{x}'(\xi_0+\chi,t)+\chi\,\partial\mathbf{x}'(\xi_0+\chi,t)/\partial\chi\,d\chi}{|\chi|^3} + \hat{\mathbf{V}}_E(k,t),$$

where now the cut-off in the inner integral is implied at $\chi = 0$ (so that $(-\delta_c c_0, \delta_c c_0)$ is removed from the range of the inner integral). Thus, since the range of this integral is now independent of ξ_0, the order of the integration can simply be changed to give (suppressing the time dependence for convenience),

$$\int_{-\infty}^{\infty} e^{ik\xi_0}d\xi_0 \int_{\substack{-\infty\\[\delta_c]}}^{\infty} \frac{\mathbf{x}'(\xi_0)-\mathbf{x}'(\xi_0+\chi)+\chi\,\partial\mathbf{x}'(\xi_0+\chi)/\partial\chi}{|\chi|^3}\,d\chi$$
$$= \hat{\mathbf{x}}(k)\int_{\substack{-\infty\\[\delta_c]}}^{\infty} \frac{(1-e^{ik\chi}-ik\chi\,e^{ik\chi})}{|\chi|^3}\,d\chi = k^2\hat{\mathbf{x}}(k)\int_{k\delta_c c_0}^{\infty} \frac{1-\cos x - x\sin x}{x^3}\,dx,$$

in view of (2.13). The integral on the right-hand side can be written in terms of cosine integral ($C_i(\eta)$) to give

$$\frac{\partial\hat{\mathbf{x}}(k,t)}{\partial t} = -2k^2\omega(k\delta_c c_0)\,\mathbf{k}\wedge\hat{\mathbf{x}}(k,t) + \frac{\hat{\mathbf{V}}_E(k,t)}{B}, \tag{2.15}\dagger$$

where

$$\omega(\eta) = \tfrac{1}{2}[(\cos\eta-1)/\eta^2 + (\sin\eta)/\eta - C_i(\eta)].$$

† It may be noted that (2.15) can be used to consider the motion of an infinitely long straight vortex filament when subjected to an arbitrary infinitesimal irrotational velocity field. In Dhanak (1980), (2.15) is used to consider the interaction between an infinitely long straight vortex and a point source and in the case of a hollow vortex the results are compared with those obtained using classical methods (see Ffowcs Williams & O'Shea (1970)). There is a good agreement between these results for $c_0/d_1 \leqslant 0{\cdot}2$, where d_1 is the non-dimensionalized distance between the position of the point source and that of the undisturbed vortex. This gives confidence in using the cut-off method in the present problem.

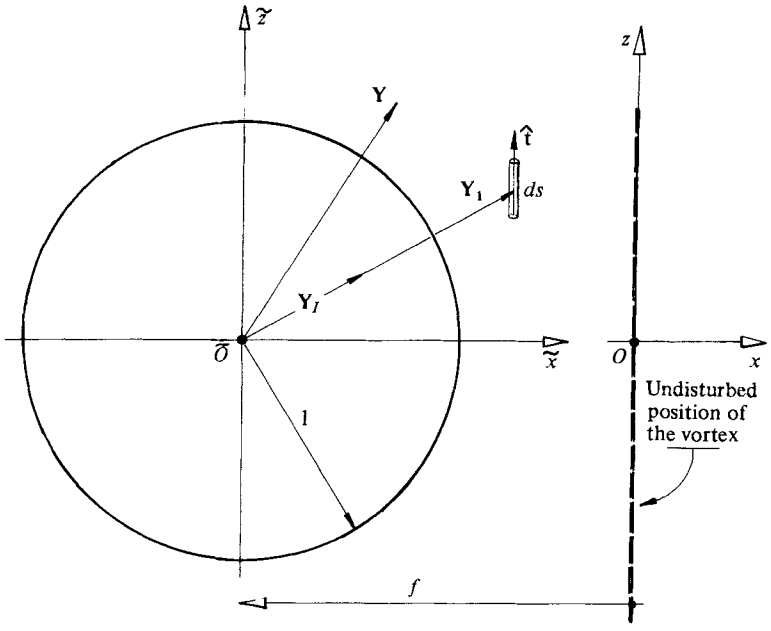

FIGURE 1. Co-ordinate system used in §§2, 4.

It now remains to obtain an expression for the velocity contribution $\mathbf{V}'_E$ before (2.15) can be solved. Suppose that, at time t^*, the centre of the sphere is at

$$\mathbf{X}_0^*(t^*) = (-f^*, 0, 0),$$

where

$$f^* = -Ut^*, \quad -\infty < t^* < \infty,$$

or in non-dimensional form

$$\mathbf{X}_0(t) = (-f, 0, 0) \tag{2.16}$$

and

$$f = -\frac{1}{B}t, \quad -\infty < t < \infty.$$

The external velocity at the vortex is due to the image vorticity in the sphere and due to the motion of the sphere. In the absence of the vortex, the velocity field at a point $\mathbf{x}^*$ can be described by the potential

$$\phi_E^*(\mathbf{x}^*) = Ua(\phi_I(\mathbf{x}) + \phi_M(\mathbf{x})), \tag{2.17}$$

where ϕ_I and ϕ_M are respectively the contributions (non-dimensional) due to the image vorticity and the motion of the sphere.

To evaluate ϕ_I when the vortex is given by its perturbed position (2.10), we write

$$\phi_I = \phi_{0I}(1 + \alpha\phi_{11} + O(\alpha^2)), \tag{2.18}$$

where ϕ_{0I} is the non-dimensional velocity potential due to the image of the undisturbed vortex in the sphere and the $O(\alpha\phi_{0I})$ terms allow for the perturbation from the straight vortex.

The potential ϕ_{0I} can be determined by as spherical harmonic analysis as follows.

In a co-ordinate frame $\tilde{O}\tilde{x}\tilde{y}\tilde{z}$, fixed with respect to the centre of the sphere, the undisturbed position of the vortex is given by $\mathbf{Y} = \overline{\mathbf{Y}}$ (see figure 1) where

$$\overline{\mathbf{Y}} = \mathbf{X}(\xi, -\infty) - \mathbf{X}_0(t) = (f, 0, \xi), \quad -\infty < \xi < \infty. \tag{2.19}$$

In the absence of the sphere, the velocity at a field point $\mathbf{Y} = (\tilde{x}, \tilde{y}, \tilde{z})$ is due to the straight vortex and the velocity potential is given by

$$\phi_0^*(\mathbf{Y}) = \frac{\Gamma}{2\pi} \tan^{-1} \frac{\tilde{y}}{\tilde{x} - f},$$

so that ($\phi_0 = \phi_0^*/Ua$)

$$\begin{aligned} \phi_0(\mathbf{Y}) &= 2B \tan^{-1} \frac{\tilde{y}}{\tilde{x} - f} \\ &= 2B \tan^{-1} \left(\frac{r \sin\theta \sin\psi}{r \sin\theta \cos\psi - f} \right), \end{aligned} \tag{2.20}$$

in terms of spherical polars (r, θ, ψ), $r^2 = \tilde{x}^2 + \tilde{y}^2 + \tilde{z}^2$. We seek the disturbance potential ϕ_{0I} when a rigid sphere is introduced. ϕ_{0I} is to satisfy the boundary condition

$$\left. \frac{\partial(\phi_0 + \phi_{0I})}{\partial r} \right|_{r=1} = 0. \tag{2.21}$$

For $r/f < 1$, ϕ_0 can be expanded in terms of spherical solid harmonics (Lamb, cha. V, 1932) as

$$\phi_0 = -2B \left\{ \frac{r \sin\theta}{f} P_1^1(\cos\theta) + \frac{r^2 \sin 2\psi}{6f^2} P_2^2(\cos\theta) + \frac{r^3 \sin 3\psi}{45 f^3} P_3^3(\cos\theta) + \ldots \right\}, \tag{2.22}$$

where $P_n^s(\mu)$ are the modified Legendre polynomials. Corresponding to each harmonic term on the right-hand side of (2.22), there exists a complementary harmonic function obtained by dividing the term by r^{2n+1}, where n is the degree of the given harmonic. ϕ_{0I} is the appropriate linear combination of these complementary functions. Thus, in view of (2.21),

$$\phi_{0I} = -2B \left\{ \frac{1}{2r^2 f} \sin\psi P_1^1(\cos\theta) + \frac{1}{9r^3 f^2} \sin 2\psi P_2^2(\cos\theta) + \frac{\sin 3\psi}{60 r^4 f^3} P_3^3(\cos\theta) + \ldots \right\},$$

or in terms of $\tilde{x}, \tilde{y}, \tilde{z}$

$$\phi_{0I} = -\frac{2B}{fr^3} \left\{ \frac{\tilde{y}}{2} + \frac{2\tilde{x}\tilde{y}}{3fr^2} + \frac{(3\tilde{x}^2 - \tilde{y}^2)}{4f^2 r^4} \tilde{y} + \ldots \right\}. \tag{2.23}$$

(Alternatively, from the sphere theorem (Weiss 1944)

$$\phi_{0I} = -2Brf\tilde{y} \int_0^1 \frac{u\,du}{(u\tilde{x} - r^2 f) + \tilde{y}^2 u^2}.)$$

The potential $\phi_M(\mathbf{Y})$ in (2.17) is given by

$$\phi_M(\mathbf{Y}) = -\frac{\mathbf{i} \cdot \mathbf{Y}}{2r^3}. \tag{2.24}$$

Thus, in the absence of the vortex, the (non-dimensional) velocity field $\mathbf{U}_E(\mathbf{Y})$ is given by $\mathbf{U}_E(\mathbf{Y}) = \nabla(\phi_M + \phi_{0I}(1 + O(\alpha))$.

In view of (2.10), the parametric equation of the perturbed vortex in $\tilde{O}\tilde{x}\tilde{y}\tilde{z}$ frame is

$$\mathbf{Y}(\xi, t) = \overline{\mathbf{Y}} + \alpha \mathbf{x}'(\xi, t) + O(\alpha^2), \tag{2.25}$$

where $\overline{\mathbf{Y}}$ is given by (2.19). Then $\mathbf{V}_E(\xi,t)\,(\equiv \mathbf{U}_E(\mathbf{Y}(\xi,t)))$ is

$$\left.\begin{aligned}\mathbf{V}_E(\xi,t) = &-\frac{B}{|\overline{\mathbf{Y}}|^3 f}\left\{\mathbf{j}\left(1+\frac{4}{3|\overline{\mathbf{Y}}|^2}+\frac{3}{2|\overline{\mathbf{Y}}|^4}+\ldots\right)+O(\alpha)\right\}\\ &-\frac{1}{2|\overline{\mathbf{Y}}|^3}\left\{\mathbf{i}-\frac{3(\mathbf{i}-\overline{\mathbf{Y}})\,\overline{\mathbf{Y}}}{|\overline{\mathbf{Y}}|^2}+O(\alpha)\right\}.\end{aligned}\right\} \tag{2.26}$$

Thus if the response of the vortex is considered on a time scale of $O(1)$ (i.e. $t^* = O(a^2/\Gamma)$) and $B = O(1)$, then it follows from (2.11) and (2.13) that $\alpha = O(1/f^3)$ (since $|\mathbf{Y}| = O(f)$), and this is required to be small in the linear analysis. Thus, since $f = f(t)$, the linear analysis will be valid provided $t \leqslant T < 0$, where T is such that

$$\alpha = \frac{1}{f_T^3} \ll 1, \tag{2.27}$$

where $f_T = |f(T)|$. Thus in (2.13),

$$\mathbf{V}'_E(\xi_0,t) = -\frac{Bf_T^3}{|\overline{\mathbf{Y}}|^3 f}\left(1+\frac{4}{3|\overline{\mathbf{Y}}|^2}\right)\mathbf{j}-\frac{f_T^3}{2|\overline{\mathbf{Y}}|^3}\left(\mathbf{i}-\frac{3(\mathbf{i}\,.\,\overline{\mathbf{Y}})\,\overline{\mathbf{Y}}}{|\overline{\mathbf{Y}}|^2}\right). \tag{2.28}$$

The contribution from the two terms in (2.28) is comparable if $f = O(B)$.

Substituting (2.28) into (2.13) and writing $\mathbf{x}' = (x', y', z')$ and using $\mathbf{x}'(\xi, -\infty) = 0$ gives

$$\alpha z'(\xi_0,t) = \frac{\xi_0}{2(\xi_0^2+t^2/B^2)^{\frac{1}{2}}}, \quad -\infty < t < T. \tag{2.29}$$

To determine $x'(\xi_0,t)$ and $y'(\xi_0,t)$, the Fourier transform of $\mathbf{V}'_E$ is taken with respect to ξ_0 and substituted into (2.15). This gives

$$\frac{\partial\hat{x}}{\partial t} = 2k^2\omega(k\delta_c c_0)\,\hat{y}+A_1(k,t), \quad \frac{\partial\hat{y}}{\partial t} = -2k^2\omega(k\delta_c c_0)\,\hat{x}+A_2(k,t), \tag{2.30}$$

where

$$\left.\begin{aligned}\alpha A_1(k,t) &= -\frac{k}{f}K_1(kf)+k^2K_2(kf),\\ \alpha A_2(k,t) &= -\frac{2B}{f}\left(\frac{k}{f}K_1(kf)+\frac{4k^2}{9f^2}K_2(kf)\right),\end{aligned}\right\} \quad k>0. \tag{2.31}$$

Here $K_m(\eta)$ is the mth-order Bessel function of the second kind.

To solve (2.30), the definition of $A_1(k,t)$ and $A_2(k,t)$ is arbitrarily extended to the range $t > T$ and the Fourier transform of (2.30) with respect to t is taken. Defining half-range Fourier transforms as

$$\begin{bmatrix}x_+^T\\ y_+^T\\ A_{1+}^T\\ A_{2+}^T\end{bmatrix} = \int_0^\infty \begin{bmatrix}\hat{x}\\ \hat{y}\\ A_1\\ A_2\end{bmatrix} e^{ist}\,dt, \quad \begin{bmatrix}x_-^T\\ y_-^T\\ A_{1-}^T\\ A_{2-}^T\end{bmatrix} = \int_{-\infty}^0 \begin{bmatrix}\hat{x}\\ \hat{y}\\ A_1\\ A_2\end{bmatrix} e^{ist}\,dt, \tag{2.32}$$

equations for (x_+^T, y_+^T) and (x_-^T, y_-^T), obtained on transforming (2.30), are solved in terms of $A_{1\pm}^T, A_{2\pm}^T$ and inverted as

$$\begin{bmatrix}\hat{x}\\ \hat{y}\end{bmatrix} = \frac{1}{2\pi}\int_{-\infty+ib}^{\infty+ib}\begin{bmatrix}x_+^T\\ y_+^T\end{bmatrix} e^{-ist}\,ds+\int_{-\infty-ic}^{\infty-ic}\begin{bmatrix}x_-^T\\ y_-^T\end{bmatrix} e^{-ist}\,ds, \tag{2.33}$$

where the paths of integration are closed in the appropriate half of the s-plane ($b, c > 0$) for inversion. Finally, $\hat{x}$ and $\hat{y}$ are inverted with respect to k to give

$$\begin{bmatrix} \alpha x'(\xi_0, t) \\ \alpha y'(\xi_0, t) \end{bmatrix} = \frac{1}{\pi} \int_0^\infty \int_0^\infty \left\{ \alpha A_1(k, t+t_1) \begin{bmatrix} \cos\hat{\theta} \\ -\sin\hat{\theta} \end{bmatrix} - \alpha A_2(k, t+t_1) \begin{bmatrix} \sin\hat{\theta} \\ \cos\hat{\theta} \end{bmatrix} \right\} \times \cos(k\xi_0)\, dt_1\, dk, \quad t < T, \tag{2.34}$$

where $\hat{\theta} = 2Bk^2\omega(k\delta_c c_0)t_1$ and αA_1 and αA_2 are given by (2.31). To evaluate the double integrals in (2.34), $k = s\cos\theta$ and $t_1 = s\sin\theta$, where $0 \leqslant s < \infty$ and $0 \leqslant \theta \leqslant \frac{1}{2}\pi$, is written and the integration carried out over s and θ variables. This means that only one of the integrals is over an infinite range.

3. Approaching sphere in the proximity of the sphere

In this section, a procedure is described for following the evolution of the vortex filament in the presence of the approaching sphere from its configuration at a time t_s ($\leqslant T < 0$), given by (2.10), (2.29) and (2.34), for times subsequent to t_s.

The evolution is followed by a step-wise numerical integration of the integro-differential equation (2.4), the contribution $\mathbf{V}_E(\xi_0, t)$ due to the evolving image system and due to the motion of the sphere being evaluated at each time step. The exact image system is discussed in § 4, where an expression for $\mathbf{V}_E$ is obtained.

The cut-off method employed in the linear analysis in § 2 to evaluate the self-induced velocity integral is inconvenient to use for numerical work. Instead, following Moore (1972), Rosenhead's method of cut-off is used here. This requires that the denominator of the integrand in the self-induced velocity line integral in (2.4) be replaced by $\{|\mathbf{X}(\xi_0, t) - \mathbf{X}(\xi, t)|^2 + \mu^2\}^{\frac{3}{2}}$, where μ is proportional to $c(\xi_0, t)$, the local radius of the core, the integration being carried out over the entire range. Thus $\mu = 2\delta_R c$. δ_R is determined in the same way as δ_c by comparing the solution using Rosenhead's cut-off method with the exact solution for a circular ring. This gives

$$\delta_R = e^{-1}\delta_c, \tag{3.1}$$

for a filament with no axial flow. For a uniform vortex,

$$\ln 2\delta_R = -\tfrac{3}{4}. \tag{3.2}$$

Now, as pointed out in § 2, the variation in core size cannot be neglected when finite amplitude disturbances are considered and a rule for evaluating c at each time step must be given. Moore & Saffman (1972) show that any variation in the internal structure along the length of the filament are smoothed out in a time which is short compared with the time scale associated with the change in the geometric configuration of the filament. Thus, on the time scale of filament motion, the (non-dimensional) core radius c and swirl velocity v are independent of position along the vortex ring. $c = c(t)$ such that the volume of the filament is conserved. Also $v = v(r_1, t)$, where r_1 is the (non-dimensional) radial distance from the axis of the filament, so that, in view of the conservation of circulation,

$$v = \frac{2}{r_1} f\left(\frac{r_1}{c}\right), \quad f(1) = 1, \tag{3.3}$$

where f is determined from the initial structure of the vortex. Thus from (2.6)

$$\frac{1}{4}\int_0^c r_1 v^2(r_1)\,dr_1 = \int_0^1 \frac{1}{\eta} f^2(\eta)\,d\eta, \tag{3.4}$$

so that δ_c and hence δ_R (see (3.1)) is constant throughout the motion, as required.

The motion of the vortex filament will be symmetrical about $z = 0$ plane so that, writing $\mathbf{X}(\xi, t) = (x, y, z)$,

$$\left.\begin{aligned} x(-\xi, t) &= x(\xi, t), \\ y(-\xi, t) &= y(\xi, t), \\ z(-\xi, t) &= -z(\xi, t), \end{aligned}\right\} \quad 0 \leqslant \xi < \infty. \tag{3.5}$$

Thus it is only necessary to follow the portion $0 \leqslant \xi < \infty$ of the filament, say, and use (3.5) to determine the shape of the remaining portion of the filament.

Thus, given an expression for $\mathbf{V}_E(\xi, t)$, the motion of the vortex can be determined by simply integrating (2.4) forward in time, calculating $\mu(t)$ at each time step. However, a method for dealing with the infinite range of the integration must be described.

It is expected that, in the time of interest, the position of those portions of the vortex which are further than a distance of a few radii of the sphere away from $z = 0$ plane will not be significantly different from that given by (2.10), (2.29) and (2.34). Thus, in view of the decay of $\mathbf{x}'$ with $\xi \to \pm\infty$, the range of the numerical integration is truncated from $(-\infty, \infty)$ to $[-A, A]$ and the portions of the vortex corresponding to $(-\infty, -A)$ and (A, ∞) are assumed to be straight and fixed in their undisturbed position. The contribution from these straight portions to the velocity at the points on the portion corresponding to $[-A, A]$ is evaluated analytically.

This method of dividing up the range of integration means that small kinks will develop at $\xi = \pm A$ and these will affect the velocity at points near $\xi = \pm A$. Thus A must be chosen so that these points are well outside the range of interest. However, the disturbance due to the kinks will propagate down the length of the vortex and the calculations must be stopped once this starts affecting the velocity at points in the range of interest. In the calculations described below, when the calculations were stopped, the disturbance due to the kinks had progressed only a short distance down the vortex and the difficulty did not arise.

Thus the self-induced velocity integral in (2.4) is written as

$$\int_{-\infty}^{\infty} \frac{\partial \mathbf{X}(\xi, t)}{\partial \xi} \wedge \frac{(\mathbf{X}(\xi_0, t) - \mathbf{X}(\xi, t)\,d\xi}{\{|\mathbf{X}(\xi_0, t) - \mathbf{X}(\xi, t)|^2 + \mu^2\}^{\frac{3}{2}}}$$

$$= \int_{-A}^{A} \frac{\partial \mathbf{X}(\xi, t)}{\partial \xi} \wedge \frac{(\mathbf{X}(\xi_0, t) - \mathbf{X}(\xi, t))\,d\xi}{(|\mathbf{X}(\xi_0, t) - \mathbf{X}(\xi, t)|^2 + \mu^2)^{\frac{3}{2}}} + \mathbf{I}_s, \tag{3.6}$$

where

$$\mathbf{I}_s(\xi, t) = \left(\int_{-\infty}^{-A} + \int_{A}^{\infty}\right) \frac{\mathbf{k} \wedge (\mathbf{X}(\xi_0, t) - \xi\mathbf{k})}{\{|\mathbf{X}(\xi_0, t) - \xi\mathbf{k}|^2 + \mu^2\}^{\frac{3}{2}}}\,d\xi$$

$$= \frac{\mathbf{k} \wedge \mathbf{X}(\xi_0, t)}{|\mathbf{X}(\xi_0, t)|^2 + \mu^2}\left(2 - \frac{A - z(\xi_0, t)}{(|\mathbf{X}(\xi_0, t) - A\mathbf{k}|^2 + \mu^2)^{\frac{1}{2}}}\right.$$

$$\left. - \frac{A + z(\xi_0, t)}{(|\mathbf{X}(\xi_0, t) + A\mathbf{k}|^2 + \mu^2)^{\frac{1}{2}}}\right). \tag{3.7}$$

Although the integrand in the cut-off integral is finite everywhere, it is large in the neighbourhood of $\xi = \xi_0$ and this would cause loss of accuracy in evaluating the integral. Thus (see Moore 1972) it is necessary to subtract off a suitable function from the integrand and write the equation of motion (2.4) as

$$\left.\begin{aligned}\frac{\partial \mathbf{X}(\xi_0,t)}{\partial t} = \int_{-A}^{A} \frac{\partial \mathbf{X}}{\partial \xi} \wedge \frac{(\mathbf{X}(\xi_0,t)-\mathbf{X}(\xi,t))}{(|\mathbf{X}(\xi_0,t)-\mathbf{X}(\xi,t)|^2+\mu^2)^{\frac{3}{2}}} - \left(\frac{\partial \mathbf{X}}{\partial \xi}\right)_0 \wedge \left(\frac{\partial^2 \mathbf{X}}{\partial \xi^2}\right)_0 P(\xi,t)\Big\} d\xi \\ + \left(\frac{\partial \mathbf{X}}{\partial \xi}\right)_0 \wedge \left(\frac{\partial^2 \mathbf{X}}{\partial \xi^2}\right)_0 \int_{-A}^{A} P(\xi,t)\, d\xi + \mathbf{I}_s(\xi_0 t) + \frac{\mathbf{V}_E(\xi_0,t)}{B},\end{aligned}\right\} \tag{3.8}$$

where

$$P(\xi,t) = \frac{\frac{1}{2}(\xi-\xi_0)^2}{((\xi-\xi_0)^2 (\partial \mathbf{X}/\partial \xi)_0^2 + \mu^2)^{\frac{3}{2}}}, \tag{3.9}$$

and $\mathbf{I}_s(\xi,t)$ is given by (3.7). The integrand in the first integral in (3.8) is $O(1)$ everywhere while the second integral is elementary.

For the nonlinear problem, the variations in core size cannot be ignored so that, in view of the uniformity of the vortex cross-section and conservation of volume,

$$\mu(t) = 2\delta_R c_0 \left\{\frac{1}{2A}\int_{-A}^{A} \left|\frac{\partial \mathbf{X}}{\partial \xi}\right| d\xi\right\}^{-\frac{1}{2}}, \tag{3.10}$$

where c_0 is the (non-dimensional) uniform core radius of the vortex filament in the undisturbed state and where the volume of the portion of the vortex corresponding to $[-A, A]$ is required to remain constant.

Since the displacement of the vortex from its undisturbed state decreases away from $z = 0$ plane (cf. (2.29)), the distribution of the Lagrangian points on the vortex can be chosen in such a way that the size of the spatial grid increases away from $\xi = 0$ point. The choice made here is

$$\xi = \operatorname{sgn}(V)\, V^2, \quad -\infty < V < \infty. \tag{3.11}$$

However, any suitable choice of function can be used. The range $[-\sqrt{A}, \sqrt{A}]$ of V was divided into three parts, $[-\sqrt{A}, -A_1]$, $[-A_1, A_1]$ and $[A_1, \sqrt{A}]$. The range $[-A_1, A_1]$ was divided into $2N_1$ portions by $2N_1+1$ equally spaced grid points. In the outer ranges, $[-\sqrt{A}, -A_1]$ and $[A_1, \sqrt{A}]$, the grid spacing was chosen to be twice that in $[-A_1, A_1]$, A being chosen so that there are $2N_2$ portions of equal length in each of the outer ranges; hence a total of $2(N_1+N_2)+1$ points per half range $[0, \sqrt{A}]$ was used. The spatial derivatives were calculated using four-point differences at all points; the particular choice of grid spacing allowed the use of the centred formulae at points near $V = \pm A_1$. Simpson's rule was used to evaluate the integrals. The integration forward in time was effected by the fourth-order Runge–Kutta formula, used because of its stability.

In § 4 an expression for $\mathbf{V}_E$ is obtained and the results of the calculations are described in § 5.

4. External velocity field

The image system of a vortex element in a sphere has been given by Lighthill (1956). This is briefly described here and an expression for the velocity field due to the image system of an infinitely long vortex is obtained.

Suppose that, with the centre of a sphere of radius a at the origin, a vortex element of length ds^* and circulation Γ is situated at $\mathbf{Y}_1^*$ (see figure 1). The strength of the element $\mathbf{J}^*$ is defined as

$$\mathbf{J}^* = \Gamma \frac{\partial \mathbf{Y}_1^*}{ds^*} ds^*. \tag{4.1}$$

Then, writing $|\mathbf{Y}_1^*| = r_1^*$, the image system of the vortex element is given by

(i) a vortex element of strength

$$\frac{2a}{r_1^*}\left(\frac{(\mathbf{J}^* . \mathbf{Y}_1^*)\,\mathbf{Y}_1^*}{r_1^{*2}} - \tfrac{1}{2}\mathbf{J}^*\right)$$

at the inverse point

$$\mathbf{Y}_I^* = \left(\frac{a}{r_1^*}\right)^2 \mathbf{Y}_1^*$$

and

(ii) a line vortex of circulation $-(\mathbf{J}^* . \mathbf{Y}_1^*)/ar_1^*$ stretching from the inverse point to the centre of the sphere.

The image system satisfies the boundary condition at the surface of the sphere and the requirement that the vorticity field inside the sphere be solenoidal. The latter condition is necessary if the corresponding Biot–Savart velocity field is to be irrotational.

For an infinitely long straight vortex filament, (i) and (ii) imply that the image system consists of a vortex ring given by $|\mathbf{Y}^* - \frac{1}{2}\mathbf{Y}_I^*| = |\frac{1}{4}\mathbf{Y}_I^*|^2$ and a vortex sheet extending over the interior of that circle (cf. Weiss 1944).

In view of (i) and (ii) the velocity at a field point $\mathbf{Y}^*$ due to the image system of a vortex element at $\mathbf{Y}_1^*$ is given by

$$\boldsymbol{\delta}\mathbf{u}^* = \frac{a}{4\pi r_1^*} \frac{(2(\mathbf{J}^* . \hat{\mathbf{Y}}_1)\hat{\mathbf{Y}}_1 - \mathbf{J}^*) \wedge (\mathbf{Y}^* - (a^2/r_1^*)\hat{\mathbf{Y}}_1)}{|\mathbf{Y}^* - (a^2/r_1^*)\hat{\mathbf{Y}}_1|^3} - \frac{(\mathbf{J}^* . \hat{\mathbf{Y}}_1)}{4\pi a} \int_0^{a^2/r_1^*} \frac{\hat{\mathbf{Y}}_1 \wedge (\mathbf{Y}^* - \lambda\hat{\mathbf{Y}}_1)}{|\mathbf{Y}^* - \lambda\hat{\mathbf{Y}}_1|^3} d\lambda, \tag{4.2}$$

where $\hat{\mathbf{Y}}_1 = \mathbf{Y}_1^*/r_1^*$. Thus in view of (4.1), in terms of the non-dimensionalized quantities ($r_1^* = ar_1$, $\mathbf{Y}^* = a\mathbf{Y}_1$, $\mathbf{ds}^* = a\mathbf{ds}$ and $\boldsymbol{\delta}\mathbf{u}^* = U\boldsymbol{\delta}\mathbf{u}$),

$$\boldsymbol{\delta}\mathbf{u} = \mathbf{W}\, ds, \tag{4.3}$$

where

$$\mathbf{W} = \frac{B}{r_1}\left[\left\{\frac{\left(2\left(\frac{\partial \mathbf{Y}_1}{\partial s} . \hat{\mathbf{Y}}_1\right)\hat{\mathbf{Y}}_1 - \frac{\partial \mathbf{Y}_1}{\partial s}\right) \wedge \left(\mathbf{Y} - \frac{\hat{\mathbf{Y}}_1}{r_1}\right)}{\left|\mathbf{Y} - \left(\frac{1}{r_1}\right)\hat{\mathbf{Y}}_1\right|^3}\right\} - \left(\frac{\partial \mathbf{Y}_1}{\partial s} . \mathbf{Y}_1\right)\hat{\mathbf{Y}}_1 \wedge \mathbf{Y} \int_0^{1/r_1} \frac{d\lambda}{|\mathbf{Y} - \lambda\hat{\mathbf{Y}}_1|^3}\right]. \tag{4.4}$$

Note that the integral in the expression is elementary.

Equation (4.3) is used here to obtain an expression for the instantaneous velocity due to the image system of the evolving infinitely long vortex filament of § 4 so that $\mathbf{Y}_1$ is given parametrically by

$$\mathbf{Y}_1 = \mathbf{X}(\xi, t) - \mathbf{X}_0(t), \quad -\infty < \xi < \infty, \quad -\infty < t < \infty, \tag{4.5}$$

where $\mathbf{X}_0(t)$ is given by (2.16). The vortex is regarded as being closed by a semi-circle of infinite radius (this is consistent with the spherical harmonic analysis of § 3 since, in obtaining the velocity potential ϕ_0 (2.20) of an infinitely long straight vortex, the same assumption is made). The velocity field is then given by $\oint \mathbf{W}\,ds$, where the integral is taken round the closed loop. However, if $\mathbf{W}$ is expanded in powers of $1/r_1$ ($r_1 > 1$) as (writing $|\mathbf{Y}| = r$)

$$\mathbf{W} = \frac{B}{r^3}\left\{\mathbf{Y}\wedge\frac{\partial\hat{\mathbf{Y}}_1}{\partial s}+\frac{1}{r_1^2}\left[\frac{\partial\mathbf{Y}_1}{\partial s}\wedge\hat{\mathbf{Y}}_1+\frac{(\mathbf{Y}.\hat{\mathbf{Y}}_1)}{r^2}\left(\frac{9}{2}\left(\frac{\partial\mathbf{Y}_1}{\partial s}.\hat{\mathbf{Y}}_1\right)(\hat{\mathbf{Y}}_1\wedge\mathbf{Y})\right.\right.\right.$$
$$\left.\left.\left.-3\left(\frac{\partial\mathbf{Y}_1}{\partial s}\wedge\mathbf{Y}\right)\right)\right]+O\left(\frac{1}{r_1^4}\right)\right\}, \quad (4.6)$$

and integrated term by term, the first term integrates to zero so that

$$\oint \mathbf{W}\,ds = \oint\left(\mathbf{W}-\frac{B}{r^3}\mathbf{Y}\wedge\frac{\partial\hat{\mathbf{Y}}_1}{\partial s}\right)ds. \quad (4.7)$$

The integrand in the integral on the right-hand side is of $O(1/R^2)$ on the semi-circular path of integration, where R is the radius of the semi-circle, so that, in the limit $R\to\infty$, integration along this path gives null contribution. Thus

$$\oint \mathbf{W}\,ds = \int_{-\infty<\xi<\infty}\left(\mathbf{W}-\frac{B}{r^3}\mathbf{Y}\wedge\frac{\partial}{\partial s}\hat{\mathbf{Y}}_1\right)ds \quad (4.8)$$

if the vortex is given by the parametric equation (4.5).

The instantaneous position of any point on the portion of the vortex filament corresponding to $-A\leqslant\xi\leqslant A$ is governed by the evolution equation (3.8). The portions corresponding to $-\infty<\xi<-A$ and $A<\xi<\infty$ are straight (see § 3) and for points on these portions $\mathbf{Y}_1$ is given by

$$\mathbf{Y}_1(\xi,t) = (-t/B,0,\xi), \quad \begin{cases}\xi\in(-\infty,-A),(A,\infty)\\ t\in(-\infty,\infty),\end{cases} \quad (4.9)$$

so that $\mathbf{ds} = (0,0,1)\,ds$.

An expression for the velocity due to the straight portions can be obtained from (4.3). After an integration by parts of the integral with respect to λ and a change of variable $\lambda = (1/r_1)\lambda_1$, the order of the integration can be changed and the integration with respect to ξ performed. Thus (4.7) becomes

$$\oint \mathbf{W}\,ds = \int_{-A<\xi<A}\left(\mathbf{W}-\frac{B}{r^3}\mathbf{Y}\wedge\frac{\partial}{\partial s}\hat{\mathbf{Y}}_1\right)ds+\mathbf{M}_s(\mathbf{Y}), \quad (4.10)$$

where $\mathbf{M}_s(\mathbf{Y})$ is the contribution from the image of the straight portions in the sphere and is given in the appendix.

Finally, in view of the motion of the sphere, the external (non-dimensional) velocity $\mathbf{U}_E(\mathbf{Y})$ at a field point $\mathbf{Y}$ in the absence of the vortex filament is given by

$$\mathbf{U}_E(\mathbf{Y}) = \oint \mathbf{W}\,ds+\nabla\phi_M, \quad (4.11)$$

where ϕ_M is given by (2.17). Then

$$\mathbf{V}_E(\xi_0,t)\equiv\mathbf{U}_E(\mathbf{Y}_0), \quad (4.12)$$

where

$$\mathbf{Y}_0 = \mathbf{X}(\xi_0, t) - \mathbf{X}_0(t), \tag{4.13}$$

and $\mathbf{Y}_1$ in (4.10) and (4.6) is given by (4.5).

5. Numerical results

To present the results, a time t_1 is defined as

$$t_1 = t - t_s, \tag{5.1}$$

where t_s ($\leqslant T < 0$) is the 'switch-over' time when the shape of the vortex is evaluated from the linear analysis of § 2 and the evolution of the vortex from this configuration is followed numerically for subsequent times.

The initial core radius was chosen as

$$c_0 \equiv \frac{c_0^*}{a} = 0{\cdot}125. \tag{5.2}$$

This allowed the evolution of the vortex to be followed using a reasonable number of grid points. The core size is not small as required by the cut-off theory since it is expected that, when the sphere is close to the vortex, the portion of the vortex which is of interest will have a radius of curvature ρ (non-dimensional) of $O(1)$. However, in the absence of axial flow, the error in the cut-off approximation is of the same order in c_0/ρ as in Saffman's (1970) formula for the velocity of a circular vortex ring. By comparing with numerical calculations of the full equations of motion, Fraenkel (1970) and Norbury (1973) have shown that Saffman's formula is fairly good for values of c_0/ρ which are not small compared with unity. Thus, although no rigorous proof is available, it is reasonable to expect that the cut-off theory will hold equally well for such values of c_0/ρ. In any case the results are not very sensitive to the value of c_0/ρ; this is because the velocity obtained by the cut-off approximation depends only logarithmically on the cut-off length and hence on the core size.

The vorticity distribution in the vortex was taken to be uniform so that δ_R is given by (3.2).

It is clear from the results (2.34) of the linear analysis that at any given time the $\xi = 0$ point will be most displaced from its undisturbed position. The y-displacement of the $\xi = 0$ point was calculated from (2.34) for various values of the ratio $1/f$, where f is as in (2.16). The double integral in (2.34) was evaluated by transforming k, t variables to s, θ variables as explained at the end of § 2. The infinite range of s was truncated to $(0, s_T)$ over which the integration was carried out using Simpson's rule. Over the range (s_T, ∞) the integrand is highly oscillatory and the integral with respect to θ is approximately evaluated using one of the standard methods used for dealing with such integrals. The results for three values of B, namely $B = 10$, 5 and 2·5, are shown in figure 2, where $|y/f|$ is plotted against $1/f$.

It was decided to follow the evolution of the vortex, subsequent to time t_s, numerically for the cases $B = 10$ and $B = 5$. The choice of t_s is made in the following way. For the two cases considered, the times $\tilde{t}_s$ when $|y/f|$ is $2\frac{1}{2}$ %, 5 % etc. is determined from figure 2. At each time, the shape of the vortex is evaluated from (2.10), (2.29) and (2.34). Using this as starting configuration of the vortex, equation (3.8) is

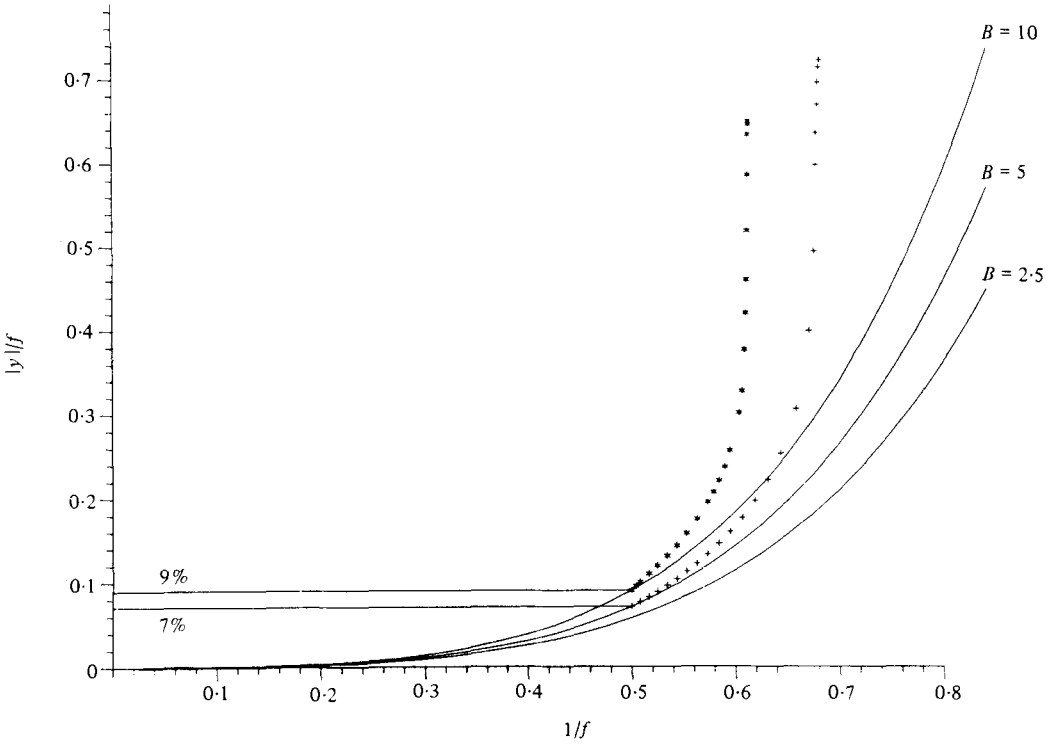

FIGURE 2. A plot of $|y|/f$ versus $1/f$. Numerical results: *, $B = 10$; +, $B = 5$. Linear theory: ——.

B	N_1	N_2	A	A_1	Δt_1
5	10	11	16·384	0·6325	0·008
10	10	11	16·384	0·6325	0·016

TABLE 1

integrated numerically over a trial period and the values of y/f obtained from the calculations are compared with the results of linear analysis. t_s is then chosen to be the maximum value of $\tilde{t}_s$ for which there is reasonable agreement between the two results over the trial period.

For both $B = 10$ and $B = 5$ cases, it was found possible to choose t_s so that y/f was 9 % at t_s. However, for convenience, t_s was chosen so that for both cases $1/f = 0{\cdot}5$. This implies

$$t_s = -2B. \tag{5.3}$$

From figure 2, $|y/f|$ is 9 % at this time for $B = 10$ case and 7 % for $B = 5$. Thus linear theory is adequate until the sphere is fairly close to the vortex.

Table 1 shows the values of N_1, N_2, A, A_1 and time step Δt_1 used in the calculations. Trial and error showed that these gave adequate accuracy.

At time $t_1 = \hat{t}_1$, shown in table 2, the centre of the core at $\xi = 0$ point was a distance $\hat{d}$ (see table 2) away from the centre of the sphere. This implies that the core of the

B	$\hat{t}_1$	$\hat{d}$	t_M	y_M	$\tilde{t}_1$
5	2·568	1·119	2·672	−1·057	2·608
10	3·600	1·123	3·710	−1·057	3·696

TABLE 2

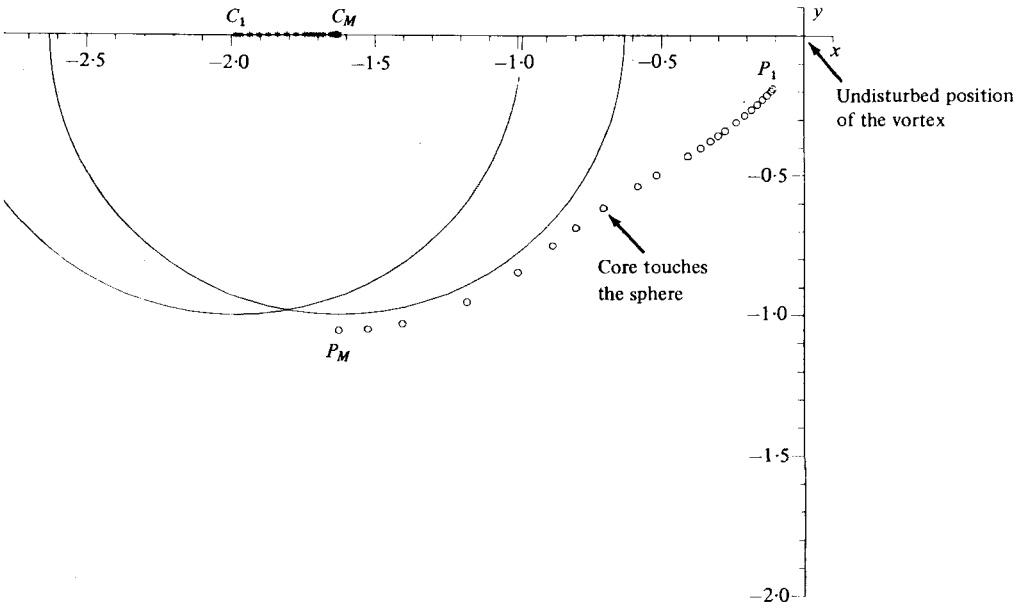

FIGURE 3. Track of $\xi = 0$ point of the vortex in the x, y plane for $B = 10$. C_1 and C_M are the positions of the centre of the sphere corresponding to the positions P_1 and P_M of the vortex. The sphere has been drawn in these two cases while for intermediate times only the centre of the sphere is shown. P_M is the position of the vortex at $t_1 = t_M$. The circulation of the vortex is in anti-clockwise sense.

vortex is touching the sphere. The situation is similar to that of two vortex filaments with their cores touching. The results at this stage may be viewed with scepticism since the calculations are based on the assumption that the separation between the vortex and its image is large. However, by means of a numerical calculation with vortices in two dimensions, in which the core was allowed for, Moore (1972) was able to show that the Biot–Savart formula gives roughly the correct velocity even when the cores are touching. In the present case, the vortex at $\xi = 0$ may be regarded as being in contact with a tangent plane and the local situation represented two-dimensionally.† Moore's study then suggests that, although the cores will be distorted so that the cut-off length will change, the approximations on which the present calculations are based will be reasonably adequate even when the vortex core is close to the sphere.

In order to determine the maximum negative y-displacement, y_M, it was decided to continue with the numerical integration up to the time $t_1 = t_M$ when this was

† An improvement on this would be to consider numerically the motion of a two-dimensional vortex of finite core round a cylinder. However, this was not attempted.

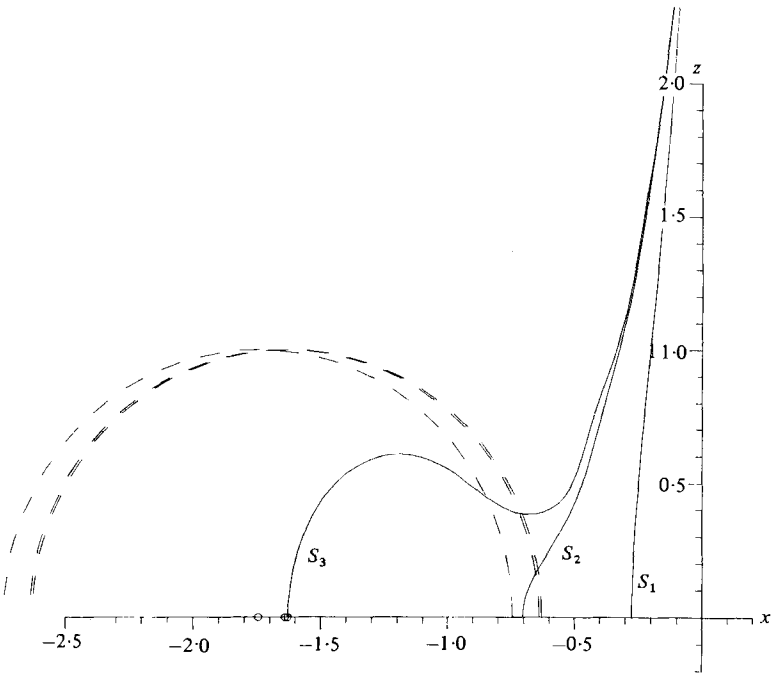

FIGURE 4. Side-view of the evolution of the vortex at time $t_1 = 2{\cdot}56(S_1)$, $t_1 = \hat{t}_1(S_2)$ and $t_1 = t_M(S_3)$ for $B = 10$. ○ marks the position of the centre of the sphere at these times. Only that portion of the filament with $0 \leqslant z(\xi, t_1) \leqslant 2{\cdot}3$ is shown.

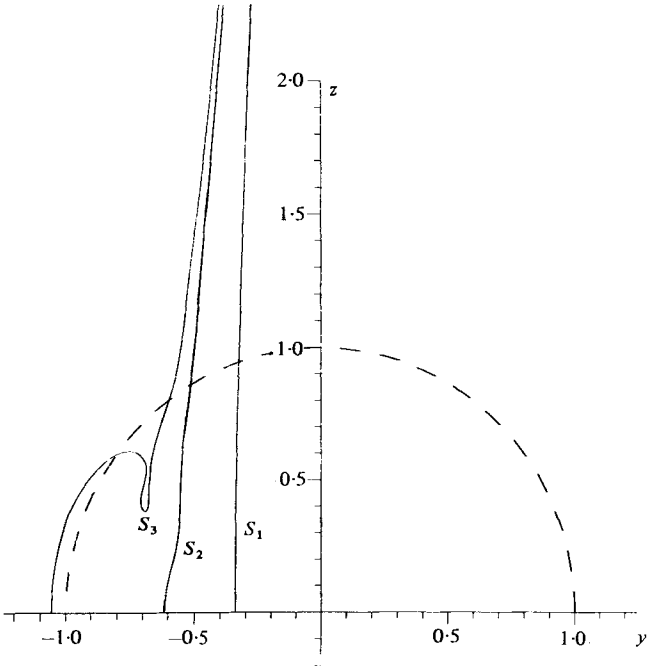

FIGURE 5. End-view of the evolution of the vortex at times $t_1 = 2{\cdot}56(S_1)$, $t_1 = \hat{t}_1(S_2)$ and $t_1 = t_M(S_3)$ for $B = 10$. Only that portion of the filament with $0 \leqslant z(\xi, t_1) \leqslant 2{\cdot}3$ is shown.

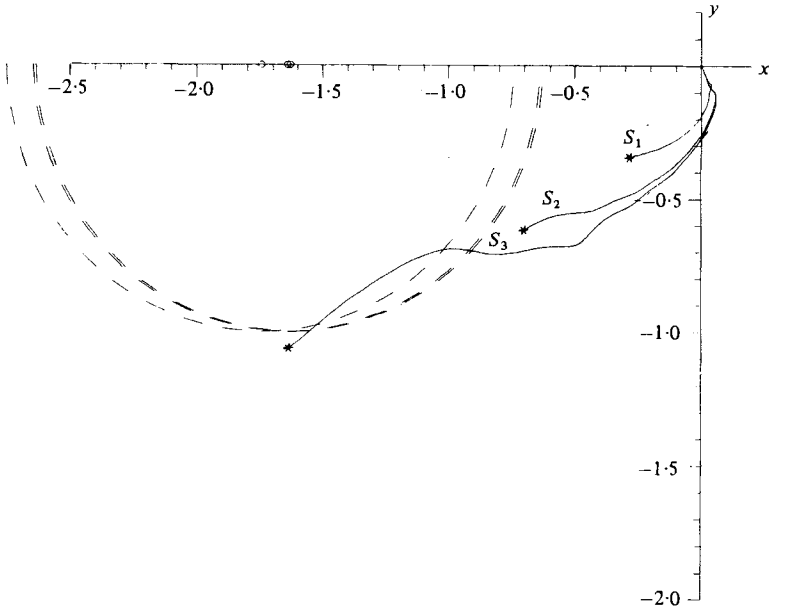

FIGURE 6. Plan-view of the vortex at times $t_1 = 2{\cdot}56(S_1)$, $t_1 = \hat{t}_1(S_2)$ and $t_1 = t_M(S_3)$ for $B = 10$. ○ marks the position of the centre of the sphere at these times. Note that in the plan view the points of the filament corresponding to $\xi \in \{(-\infty, -A) \cup (A, \infty)\}$ are mapped onto (0, 0). ✱ indicates the position of the point corresponding to $\xi = 0$.

achieved. $|y_M|$ was maximum when the x-coordinate of $\xi = 0$ point coincided with the x-co-ordinate of the centre of the sphere. The values of y_M and t_M are shown in table 2.

The position of the portion of the vortex near $z = 0$ plane, due to its proximity to the sphere, changes rapidly while points on the vortex a distance further than 1 from the $z = 0$ plane are displaced by a small amount. At $t_1 = \bar{t}_1$ (see table 2) numerical instability became established in the neighbourhood of the $z = 0$ plane, presumably because of the rapid changes there and because the distance between the grid points is not small compared with the separation between the vortex centre and the image. To cure this, the calculations were stopped at $t_1 = \bar{t}_1 - 2\Delta t_1$ and restarted with more points so that the grid spacing was reduced by half and the time step was taken to be $\frac{1}{4}\Delta t_1$. This removed the instability.

In figure 2 various values of $|y/f|$ for times subsequent to t_s are shown for the two cases considered and compared with the corresponding results of linear analysis. The results from the numerical calculations are shown up to the time when $|y/f|$ achieves a maximum value. For subsequent times the value of $|y/f|$ drops. The reason may be apparent from figure 3 which shows the track of $\xi = 0$ point in the x–y plane for the case $B = 10$. As the vortex 'clears' the sphere at time $t_1 = t_M$ the vortex appears to follow a roughly circular path round the sphere. This is confirmed by integration over a few additional time steps which show that the magnitude of the y-displacement falls for $t_1 > t_M$. To follow the motion of the vortex for subsequent times, more grid points and smaller time steps are necessary. However, in view of the dubious significance of the results at this stage, this was not done.

In figure 4 three views of the side elevations at different stages of the evolution are shown for the $B = 10$ case while figure 5 shows the corresponding end elevations. Only the portion of the filament near $z = 0$ for $z > 0$ is shown in the figures. The figures clearly show the rapid change in shape of the vortex near $z = 0$ plane subsequent to time $t_1 = \hat{t}_1$. The plan view is shown in figure 6; the asterisk indicates the position of the point on the filament corresponding to $\xi = 0$. At any instant this point is displaced furthest from the undisturbed position $(0, 0)$.

In both $B = 5$ and $B = 10$ cases, the overall increase in length of the portion of the vortex considered increased by less than 1·5 %. The vortex stretched most in the neighbourhood of $\xi = 0$ point where, in the $B = 10$ case, the distance between two points, initially a distance δz apart, increased to $1{\cdot}3\delta z$ at $t_1 = \hat{t}_1$ and to $5\delta z$ at $t_1 = t_M$. The corresponding values in $B = 5$ case were similar. Away from $\xi = 0$ points, certain portions of the vortex underwent contraction.

At $t = t_M$ the kinks at $\xi = \pm A$ due to the truncation of the vortex had progressed by a distance less than 1 down the length of the vortex and did not affect the velocity at points on the vortex a distance less than 5 from $z = 0$ plane.

A qualitative experiment was conducted in a cylindrical tank of water in which a 'bathtub vortex' was set up at the centre. From the edge of the tank, a sphere was moved towards the vortex at a speed corresponding to $B = 10$. Dye was used for flow visualization.

The vorticity distribution in the bathtub vortex is not uniform. However, it is expected that this will make only a quantitative difference to the motion of the vortex.

As anticipated here, the vortex does not move appreciably until the sphere is quite close to the vortex, when it commences to move in the sense indicated in figure 5. However, the cross stream induced by the vortex over the sphere produces a side wake in the region into which the vortex is starting to move. The wake appears to interact strongly with the vortex filament, which soon breaks up.

Thus the present calculations are of approximate validity in real fluids since viscous diffusion and the wake of the sphere have been excluded in the calculations.

I am grateful to Professor D. W. Moore for suggesting the problem and for his encouragement and advice. During the preparation of this paper, I was financially supported by the Science Research Council.

Appendix. Velocity contribution from the image of the straight portions of the vortex filament in the sphere

Here an expression for $\mathbf{M}_s(\mathbf{Y})$ in (4.10) is written down. By integrating the integrand on the right-hand side of (4.8) over $\xi \in (-\infty, -A)$ and $\xi \in (A, \infty)$ in the manner described in § 4, we have

$$\mathbf{M}_s(\mathbf{Y}) = \frac{B}{r^3}\left\{\mathbf{Y} \wedge \left[\left(f^2\hat{A}_{10}(1) + 2 - \frac{2A}{(f^2+A^2)^{\frac{1}{2}}}\right)\mathbf{k} - f\hat{A}_{11}(1)\,\mathbf{i}\right] + f\hat{A}_{10}(1)\,\mathbf{j}\right.$$
$$+ \frac{3}{r^2}\mathbf{Y} \wedge \int_0^1 [(\mathbf{Y}\,.\,\mathbf{k})\,(\hat{A}_{22}(\lambda) f\mathbf{i} + \hat{A}_{23}(\lambda)\,\mathbf{k}) + (\mathbf{Y}\,.\,\mathbf{P}(\lambda))\,(\hat{A}_{21}(\lambda) f\mathbf{i}$$
$$\left. + \hat{A}_{22}(\lambda)\,\mathbf{k})]\,d\lambda\right\}. \quad \text{(A 1)}$$

Here

$$\mathbf{P}(\eta) = f\mathbf{i} - \frac{\eta}{r}\hat{\mathbf{Y}},$$

f is as in (2.16) and $\hat{A}_{nm}(\eta)$ are given by:

$$\hat{A}_{n,m}(\eta) = \sum_{k=0}^{m} \frac{m!\,(2n-k-1)!}{2n!\,(m-k)!}\left[\frac{(A)^{m-k}}{(A \pm |\mathbf{P}(\eta)|)^{2n-k}} - \frac{(-A)^{m-k}}{(-A \pm |\mathbf{P}(\eta)|)^{2n-k}}\right], \begin{cases} n = 1, 2, \ldots, \\ m = 0, 1, 2, \ldots, \end{cases}$$

if $\mathbf{k}\,.\,\mathbf{P}(\eta) = \pm|\mathbf{P}|$. If $|\mathbf{k}\,.\,\mathbf{P}(\eta)| \neq |\mathbf{P}|$, i.e. $|\mathbf{k} \wedge \mathbf{P}| \neq 0$, then

$$\hat{A}_{2,m}(\eta) = \frac{1}{(4-m)}\left\{\left[\frac{A^2}{|A\mathbf{k}+\mathbf{P}(\eta)|^3} - \frac{A^2}{|-A\mathbf{k}+\mathbf{P}(\eta)|^3}\right] + (2m-5)\,\mathbf{k}\,.\,\mathbf{P}(\eta)\,\hat{A}_{2,m-1} + (m-1)\,|\mathbf{P}|^2\,\hat{A}_{2,(m-2)}\right\}, \quad m = 1, 2, 3,$$

$$\hat{A}_{2,0}(\eta) = \frac{1}{3|\mathbf{k} \wedge \mathbf{P}(\eta)|^2}\left[\frac{A+\mathbf{k}\,.\,\mathbf{P}}{|A\mathbf{k}+\mathbf{P}(\eta)|^3} + \frac{A-\mathbf{k}\,.\,\mathbf{P}}{|-A\mathbf{k}+\mathbf{P}(\eta)|^3} + 2\hat{A}_{1,0}\right],$$

$$\hat{A}_{1,1}(\eta) = \frac{1}{|\mathbf{k} \wedge \mathbf{P}(\eta)|^2}\left[\frac{|\mathbf{P}(\eta)|^2 + A\mathbf{k}\,.\,\mathbf{P}(\eta)}{|A\mathbf{k}+\mathbf{P}(\eta)|} - \frac{|\mathbf{P}|^2 - A\mathbf{k}\,.\,\mathbf{P}}{|-A\mathbf{k}+\mathbf{P}(\eta)|}\right],$$

$$\hat{A}_{1,0}(\eta) = \frac{1}{|\mathbf{k} \wedge \mathbf{P}(\eta)|^2}\left[\frac{A+\mathbf{k}\,.\,\mathbf{P}(\eta)}{|A\mathbf{k}+\mathbf{P}(\eta)|} + \frac{A-\mathbf{k}\,.\,\mathbf{P}(\eta)}{|-A\mathbf{k}+\mathbf{P}(\eta)|}\right].$$

Putting $A = 0$ in (A 1), we obtain the velocity due to the image system of an infinitely long straight vortex. The result is in agreement with that given by Weiss (1944) for this case; Weiss obtained the result using his sphere theorem. Note that the sphere theorem is inconvenient to use in the present nonlinear problem since it requires evaluating the velocity potential of the evolving vortex at each time step.

As a further check, putting $A = 0$ in (A 1) and expanding $\mathbf{M}_s$ in powers of $1/r^2$ gives a result in agreement with the spherical harmonic analysis of § 2.

REFERENCES

Crow, S. C. 1970 *A.I.A.A. J.* **8**, 1972.

Dhanak, M. R. 1980 Ph.D. thesis, University of London.

Ffowcs Williams, J. E. & O'Shea, S. 1970 *J. Fluid Mech.* **14**, 257.

Fraenkel, L. E. 1970 *Proc. Roy. Soc.* A **316**, 29.

Lamb, H. 1932 *Hydrodynamics*. Dover.

Lighthill, M. J. 1956 *Proc. Camb. Phil. Soc.* **52**, 317.

Moore, D. W. 1972 *Aeronaut. Quart.* **23**, 307.

Moore, D. W. & Saffman, P. G. 1971 *Aircraft Wake Turbulence* (ed. J. H. Olsen, A. Goldberg & M. Rogers), p. 339. Plenum.

Moore, D. W. & Saffman, P. G. 1972 *Phil. Trans. Roy. Soc.* A **272**, 403.

Norbury, J. 1973 *J. Fluid Mech.* **57**, 417.

Raja Gopal, E. S. 1963 *Ann. Phys.* **25**, 196.

Saffman, P. G. 1970 *Stud. Appl. Math.* **49**, 371.

Weiss, P. 1944 *Proc. Camb. Phil. Soc.* **40**, 259.

Widnall, S. E., Bliss, D. & Zalay, A. 1971 *Aircraft Wake Turbulence* (ed. J. H. Olsen, A. Goldberg & M. Rogers), p. 305. Plenum.